Supporting Information: Direct Conversion of Natural Tissues and Food Waste into Aerogels and Application in Oleogelation

Lara Gibowsky[a,e] 0000-0001-6359-9426, Lorenzo De Berardinis[c] 0000-0001-6058-9863, Stella Plazzotta[c] 0000-0001-6152-4316, Erik Manke[a], Isabella Jung[a] 0000-0002-7076-0721, Daniel Alexander Méndez[d] 0000-0001-6414-305X,Finnja Heidorn[a], Gesine Liese[b] 0009-0001-6906-4577, Julia Husung[b], Andreas Liese[b,e] 0000-0002-4867-9935, Pavel Gurikov[a,f] 0000-0003-0598-243X ,Irina Smirnova[a,e] 0000-0003-4503-4039, Lara Manzocco[c] 0000-0002-7853-7823, Baldur Schroeter[, a,e] 0000-0002-2577-055X*

[a] Institute of Thermal Separation Processes, Hamburg University of Technology, Eißendorfer Straße 38, 21073 Hamburg, Germany

[b] Institute of Technical Biocatalysis, Hamburg University of Technology, Denickestraße 15, 21073 Hamburg, Germany

[c] Department of Agricultural, Food, Environmental and Animal Sciences, University of Udine, Via Sondrio 2/A, 33100 Udine, Italy

[d] Food Safety and Preservation Department, Institute of Agrochemistry and Food Technology (IATA-CSIC), Valencia, Spain

[e] United Nations University Hub on Engineering to Face Climate Change at the Hamburg University of Technology, United Nations University Institute for Water, Environment and Health (UNU-INWEH), Hamburg, Germany

[f] aerogel-it GmbH, Albert-Einstein-Str. 1, 49076 Osnabrück, Germany

[*] *Corresponding author, email:* baldur.schroeter@tuhh.de

Table S1: Sample list, categorization and different physical properties of supercritically dried tissues. ρ_b = bulk density, ρ_s = skeletal density, S_m = specific surface area, V_{meso} = meso pore volume, C = BET constant.

Sample category	Material (-)	ρ_{bulk}* (g cm^{-3})	ρ_s** (g cm^{-3})	S_m (m^2 g^{-1})	V_{meso} (cm^3 g^{-1})	R^2 BET (-)	C (-)
1	Radish	0.016	1.63 ± 0.02	328	0.654	0.9998	58
	Apple	0.021	1.85 ± 0.08	202	0.550	0.9999	87
	Bell pepper	0.061	1.51 ± 0.02	190	0.311	0.9999	62
	Carrot	0.044	1.49 ± 0.02	125	0.274	0.9999	182
	Cucumber	0.008	n.d.	238	0.589	0.9999	128
2	Mushroom *Agaricus*	0.009	n.d.	281	0.775	0.9999	60
	Banana peel	0.069	1.46 ± 0.01	240	0.429	0.9998	59
	Pear	0.050	1.43 ± 0.02	168	0.526	0.9998	148
	Plum	0.024	n.d.	259	0.933	0.9999	123
	Tomato	0.024	2.39 ± 0.06	251	0.742	0.9990	37
	Orange peel	0.071	1.65 ± 0.02	285	1.146	0.9999	106
	Onion	0.031	1.62 ± 0.02	108	0.302	0.9999	74
3	Kiwi	0.013	2.08 ± 0.06	354	2.560	0.9999	86
	Orange	0.018	2.33 ± 0.02	322	1.363	0.9999	68
	Honey Pomelo	0.042	1.49 ± 0.034	305	1.245	0.9999	87
	Strawberry	0.030	n.d.	277	0.942	0.9996	47
	Nectarine	0.028	1.60 ± 0.02	248	1.325	0.9999	52
not categorized	Sweet potato	0.120	1.50 ± 0.01	n.d.	n.d.	0.9982	27
	Watermelon	0.025	n.d.	n.d.	n.d.	0.9994	-302275
	Eggplant	0.028	1.47 ± 0.01	n.d.	n.d.	0.9990	37

* Measured deviations of all samples are below 5% for threefold determinations.

** Fourfold determinations.

Table S2: Composition of supercritically dried samples with corresponding standard deviations (n = 3). The amount of all individual components of the is given in mg mg^{-1} of the soluble fraction. The ash content is given as % regarding the overall sample dry mass.

Material [-]	Cellulose	Protein	Monosaccharides/Sugar acids			Pectin fraction					
			Glucuronic acid	Glucose	Mannose	Galacturonic acid	Arabinose	Fucose	Galactose	Rhamnose	Xylose
Radish	0.129 ± 0.024	0.147 ± 0.003	0.003 ± 0.001	0.054 ± 0.008	0.015 ± 0.003	0.352 ± 0.044	0.079 ± 0.012	0.003 ± 4.5 e-5	0.065 ± 0.008	0.043 ± 0.006	0.037 ± 0.006
Apple	0.175 ± 0.031	0.039 ± 0	0.002 ± 0	0.0945 ± 0.017	0.021 ± 0.004	0.333 ± 0.045	0.205 ± 0.025 ±	0.010 ± 0.001	0.121 ± 0.017	0.034 ± 0.004	0.093 ± 0.012
Bell pepper	0.276 ± 0.021	0.119 ± 0.001	0.003 ± 0	0.037 ± 0.007	0.014 ± 0.002	0.289 ± 0.012	0.025 ± 0.002	0.001 ± 0	0.028 ± 0.004	0.020 ± 0.002	0.034 ± 0.003
Carrot	0.271 ± 0.019	0.089 ± 0.003	0.003 ± 0	0.054 ± 0.006	0.014 ± 0.001	0.243 ± 0.020	0.056 ± 0.002	0.001 ± 0	0.118 ± 0.003	0.032 ± 0.001	0.012 ± 0
Mushroom*	0 ± 0	0.429 ± 0.001	0.013 ± 0.001	0.274 ± 0.028	0.027 ± 0.003	0.007 ± 0.002	0.017 ± 0.002	0.002 ± 0.001	0.011 ± 0.001	0.002 ± 0.001	0.017 ± 0.001
Banana peel	0.094 ± 0.030	0.073 ± 0.001	0.018 ± 0.001	0.120 ± 0.007	0.029 ± 0.002	0.134 ± 0.006	0.088 ± 0.002	0.001 ± 0	0.032 ± 0.001	0.007 ± 0	0.090 ± 0.004
Cucumber	0.225 ± 0.033	0.135 ± 0.018	0.008 ± 0.002	0.022 ± 0.002	0.013 ± 0.002	0.176 ± 0.016	0.019 ± 0.002	0 ± 0	0.028 ± 0.002	0.013 ± 0.002	0.044 ± 0
Pear	0.117 ± 0.017	0.046 ± 0	0.002 ± 0.001	0.025 ± 0.004	0.0087 ± 0.001	0.250 ± 0.008	0.244 ± 0.019	0.005 ± 0	0.066 ± 0.004	0.021 ± 0.001	0.055 ± 0.007
Plum	0.185 ± 0.020	0.083 ± 0.002	0.005 ± 0.001	0.028 ± 0.002	0.012 ± 0.001	0.340 ± 0.050	0.048 ± 0.008	0.005 ± 0.001	0.113 ± 0.019	0.026 ± 0.004	0.037 ± 0.005
Tomato	0.325 ± 0.017	0.069 ± 0.001	0.005 ± 0.001	0.046 ± 0.008	0.030 ± 0.005	0.277 ± 0.016	0.042 ± 0.002	0.001 ± 0.001	0.032 ± 0.002	0.027 ± 0.002	0.062 ± 0.005
Orange peel	0.103 ± 0.044	0.038 ± 0.001	0 ± 0	0.023 ± 0.014	0.018 ± 0.003	0.283 ± 0.028	0.149 ± 0.025	0.006 ± 0.001	0.118 ± 0.008	0.027 ± 0.004	0.039 ± 0.006
Onion	0.174 ± 0.021	0.088 ± 0.001	0.001 ± 0	0.027 ± 0.003	0.008 ± 0.001	0.270 ± 0.017	0.018 ± 0.002	0.004 ± 0	0.313 ± 0.026	0.020 ± 0.001	0.026 ± 0.001
Kiwi	0.187 ±	0.136 ±	0.011 ±	0.048 ±	0.023 ±	0.213 ±	0.022 ±	0.006 ±	0.116 ±	0.020 ±	0.094 ±

	0.035	0	0	0.008	0.004	0.055	0.005	0.002	0.024	0.004	0.016
Orange	0.104 ± 0.013	0.076 ± 0.008	0.010 ± 0	0.015 ± 0.005	0.014 ± 0.005	0.298 ± 0.060	0.157 ± 0.032	0.004 ± 0.001	0.089 ± 0.014	0.02 ± 0.003	0.026 ± 0.009
Honey Pomelo	0.207 ± 0.024	0.114 ± 0.003	0.003 ± 0.001	0.028 ± 0.003	0.019 ± 0.002	0.426 ± 0.046	0.200 ± 0.020	0.004 ± 0	0.044 ± 0.005	0.025 ± 0.002	0.037 ± 0.009
Strawberry	0.122 ± 0.012	0.129 ± 0.002	0.004 ± 0	0.031 ± 0.002	0.010 ± 0.001	0.289 ± 0.015	0.060 ± 0.004	0.005 ± 0	0.065 ± 0.008	0.022 ± 0.001	0.051 ± 0.004
Nectarine	0.243 ± 0.009	0.139 ± 0.001	0.005 ± 0	0.039 ± 0.004	0.018 ± 0.002	0.172 ± 0.009	0.115 ± 0.002	0.007 ± 0	0.067 ± 0.003	0.022 ± 0.001	0.063 ± 0.005
Sweet potato	0.161 ± 0.036	0.063 ± 0	0 ± 0	0.618 ± 0.012	0 ± 0	0.034 ± 0.001	0.014 ± 0	0 ± 0	0.027 ± 0	0.007 ± 0	0.009 ± 0
Watermelon	0.230 ± 0.006	0.077 ± 0.001	0.002 ± 0	0.034 ± 0.006	0.008 ± 0.002	0.336 ± 0.022	0.0881 ± 0.001	0.006 ± 0	0.035 ± 0.002	0.015 ± 0.001	0.089 ± 0.005
Eggplant	0.231 ± 0.003	0.088 ± 0.001	0.002 ± 0	0.040 ± 0.012	0.014 ± 0	0.281 ± 0.030	0.028 ± 0.016	0.001 ± 0	0.073 ± 0.030	0.024 ± 0.006	0.051 ± 0.016

*The mushroom is the only natural tissue-based sample with a chitin content (0.330 ± 0.026 mg mg^{-1}).

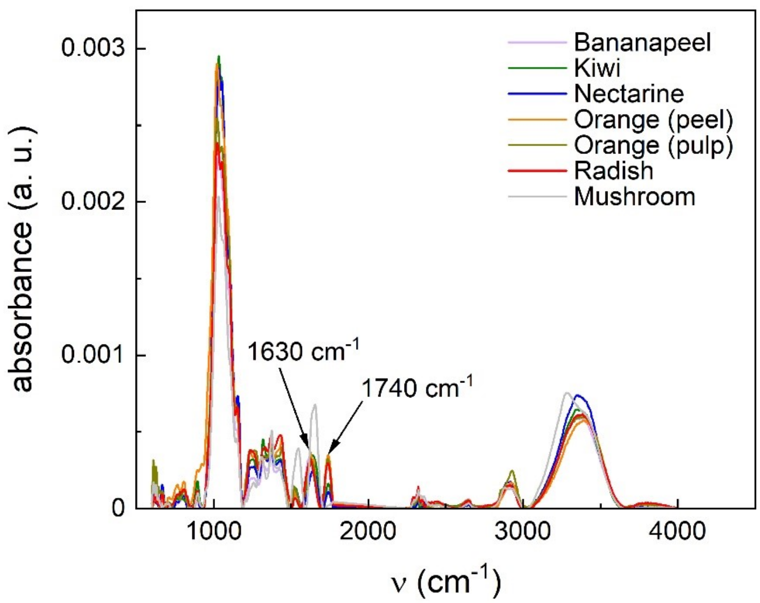

Figure S1: FT-IR spectra of tissue based aerogels which were used for oleogelation. The highlighted bands were used to estimate the %DM.

FT-IR spectra show the signals of the most significant components: pectin[1], cellulose[2] and chitin[3] in case of the mushroom sample. The spectra of all samples with exception of the mushroom based tissue were highly similar and are therefore discussed collectively. In all cases, a complex signal is visible in the fingerprint region, which ranges from of ~ 900 – 1200 cm^{-1}. While it is difficult to assign the individual bands in this region to single corresponding vibrational modes, they can be generally attributed to C-OH deformation vibration, C-C stretching vibrations and to the C-O-C glyosidic linkage of pectin as well to the C–O–C pyranose ring skeletal vibration of cellulose.[1], [2] The bands at 1630 cm^{-1} (C=O stretching vibration) and 1740 cm^{-1} (COO stretching vibration) were used to determine the %DM of the pectins of different samples (see main text, eq. 4).[1] Further signals attributed to cellulose were determined at 897 cm^{-1} (β-glycosidic linkages) and 2914 cm^{-1} (C-H stretching).[2] The broad signal in the range of 3050 – 3635 cm^{-1} is attributed to -O-H stretching.[2] For the mushroom sample, characteristic peaks of chitin were found: The adsorption band at 1310 cm^{-1} corresponds most probably to amide II (N-H bending) and at 1548 cm^{-1} to amide III (C-N stretching). The bands at 1624 cm^{-1} and 1659 cm^{-1} largely overlap and represent the amide I stretching featuring different hydrogen-bond based interactions with neighbored functionalities.[3] The broad signal in the range of 3050 – 3635 cm^{-1} is attributed to NH_2 and -OH stretching vibrations.

Reference list for analysis of IR-Spectra

[1] E. L. La Cava, E. Gerbino, S- C- Sgroppo, A- Gómez-Zavaglia, *J. Food Sci.*, 2018, **83(6)**, 1613 -1621.

[2] W. Chen, H. He, H. Zhu, M. Cheng, Y. Li, S. Wang, *Polymers*, 2018, **10**, 592.

[3] E. M. Dahmane, M. Taourirte, N. Eladlani, M. Rhazi, *Int. J. Polym. Anal. Charact.*, 2014, **19**, 342 -351.

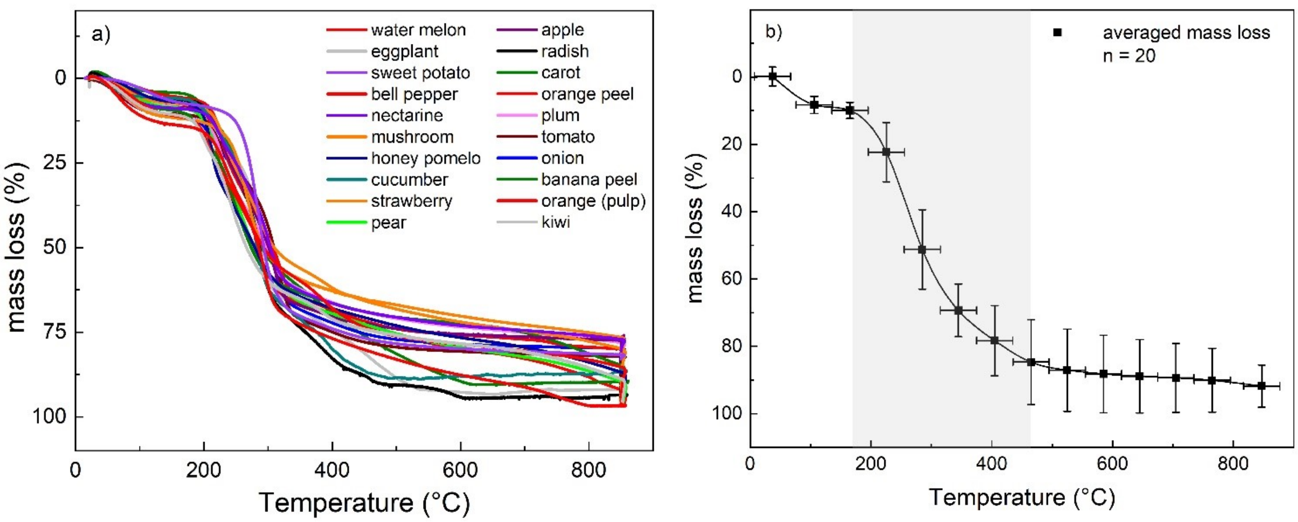

Figure S2: Thermal decomposition curves of all powders obtained after supercritical drying, determined under oxidizing atmosphere. (a) all single sample curves, (b) course of the averaged values. The y-error corresponds the standard deviation of the averaged values and the x-error to the tolerance of the average. The grey zone represents the temperature range of most pronounced mass loss (biopolymer decomposition).

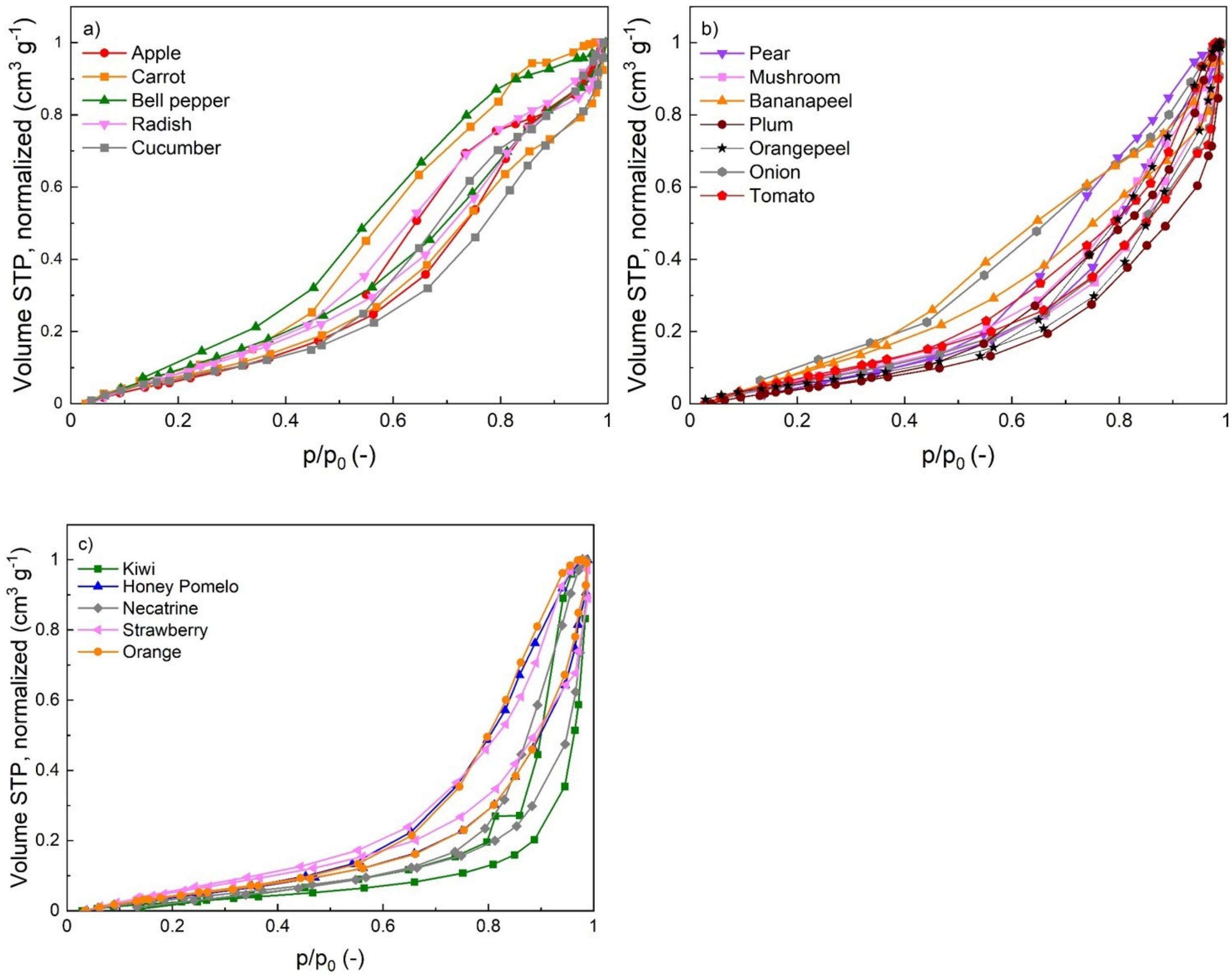

Figure S3: Normalized nitrogen-adsorption-desorption isotherms for tissue based samples of categories 1 (a), 2 (b) and 3 (c).

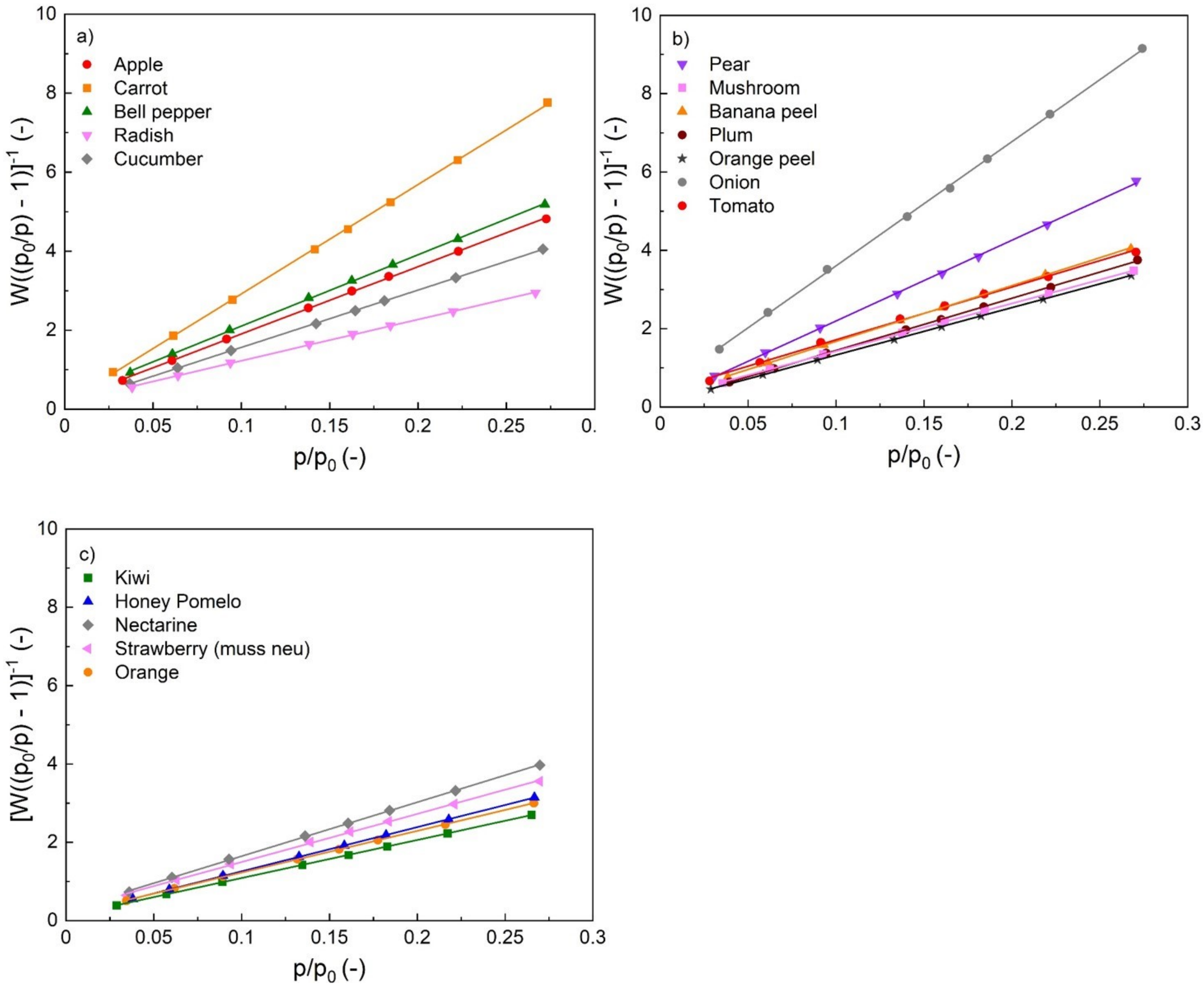

Figure S4: BET plots derived from isotherms shown in figure S1 for samples of categories 1 (a), 2 (b) and 3 (c).

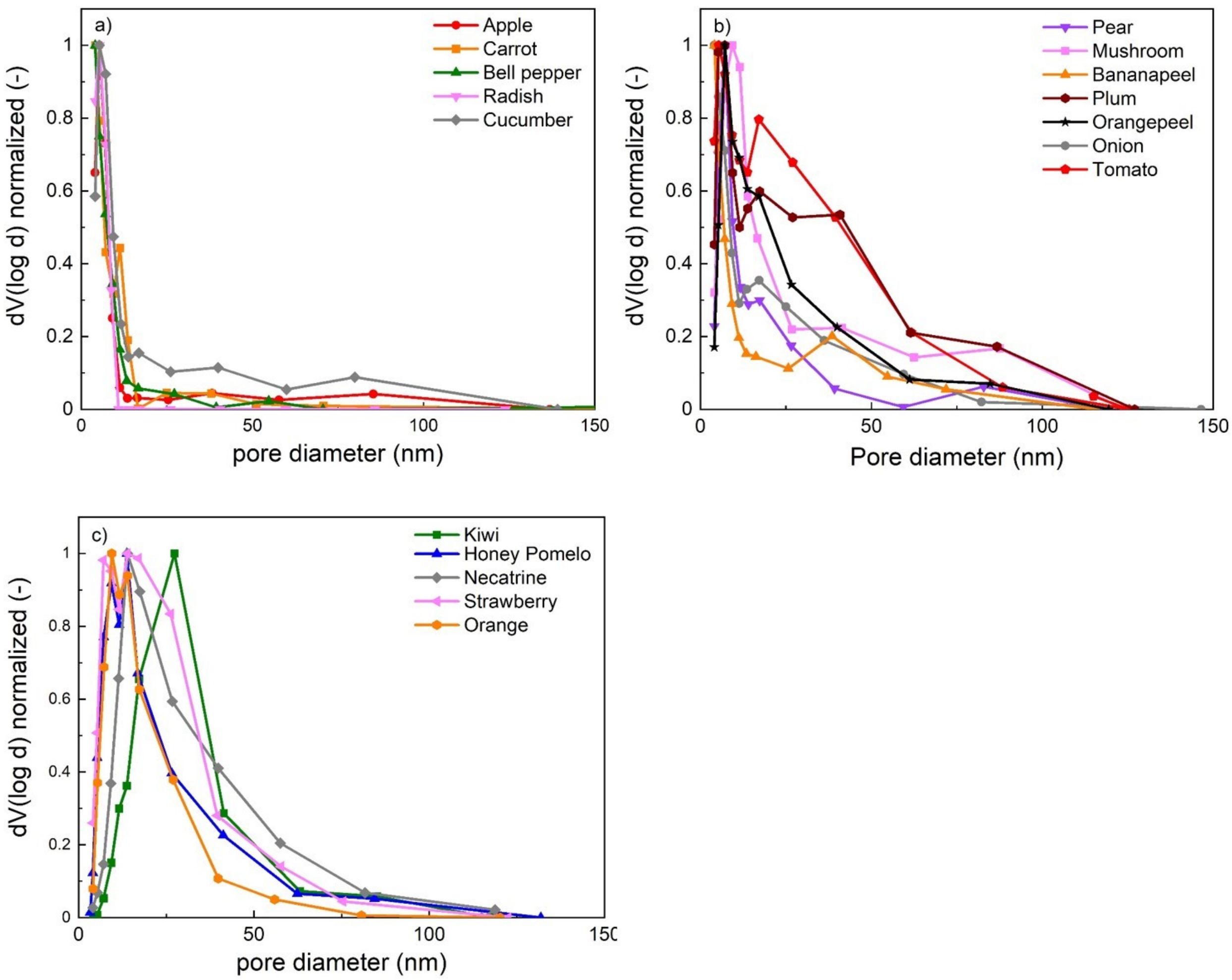

Figure S5: Normalized pore size distributions derived from isotherms shown in figure S1 for samples of categories 1 (a), 2 (b) and 3 (c).

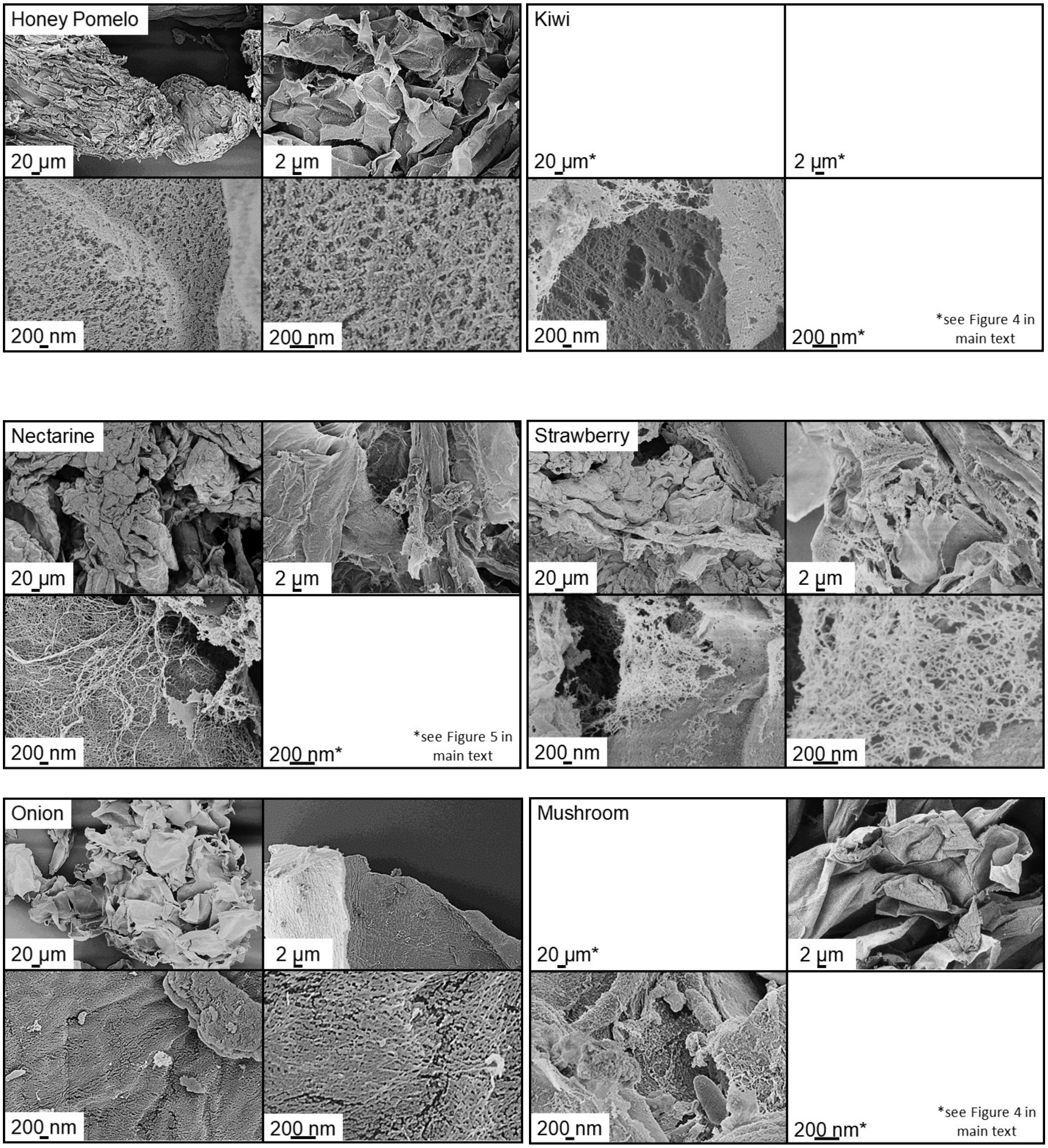
Honey Pomelo
20 µm
2 µm
200 nm
200 nm
Kiwi
20 µm*
2 µm*
200 nm
200 nm*
*see Figure 4 in main text
Nectarine
20 µm
2 µm
200 nm
200 nm*
*see Figure 5 in main text
Strawberry
20 µm
2 µm
200 nm
200 nm
Onion
20 µm
2 µm
200 nm
200 nm
Mushroom
20 µm*
2 µm
200 nm
200 nm*
*see Figure 4 in main text

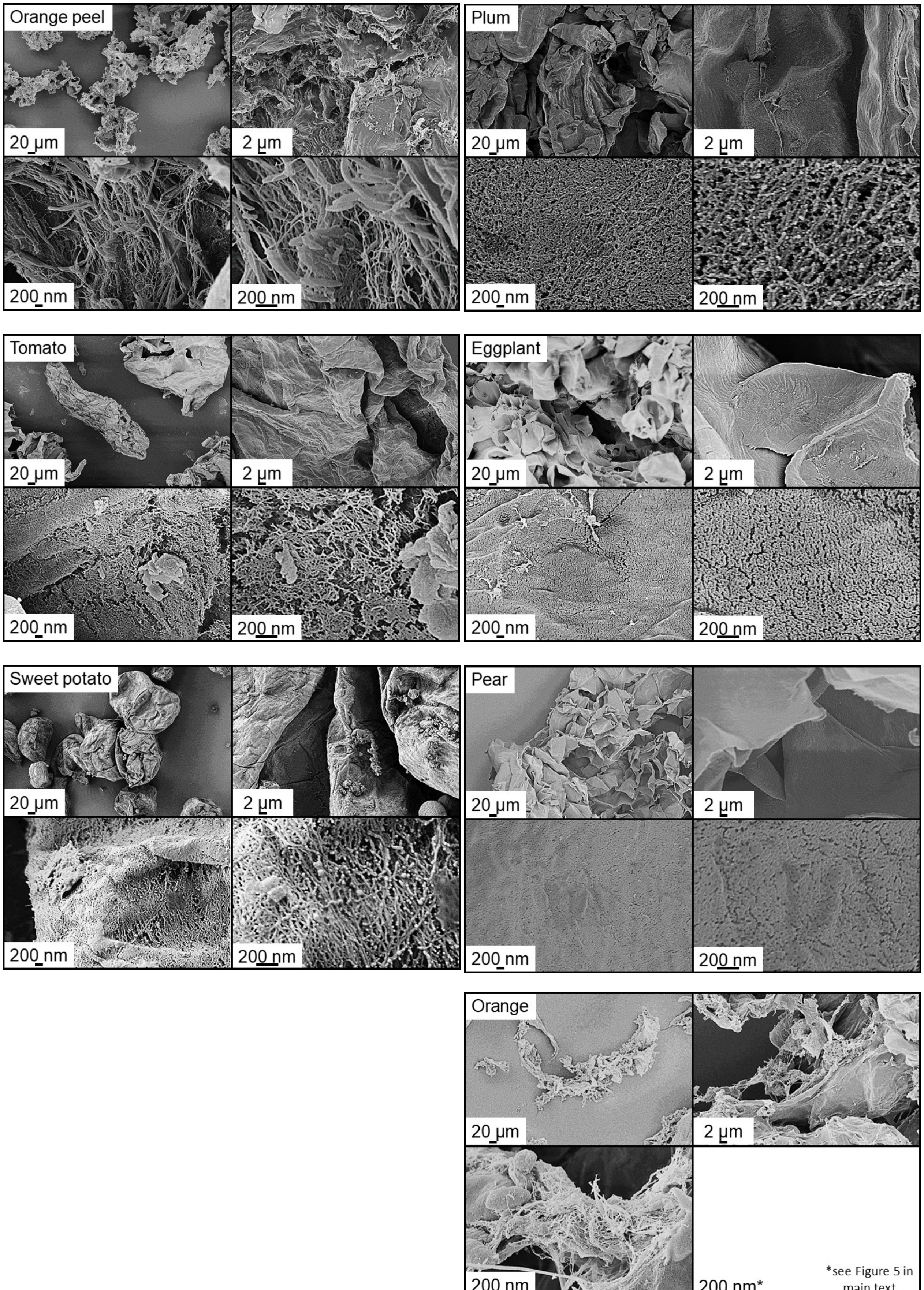
Orange peel
20 µm
2 µm
200 nm
200 nm
Plum
20 µm
2 µm
200 nm
200 nm
Tomato
20 µm
2 µm
200 nm
200 nm
Eggplant
20 µm
2 µm
200 nm
200 nm
Sweet potato
20 µm
2 µm
200 nm
200 nm
Pear
20 µm
2 µm
200 nm
200 nm
Orange
20 µm
2 µm
200 nm
200 nm*
*see Figure 5 in main text

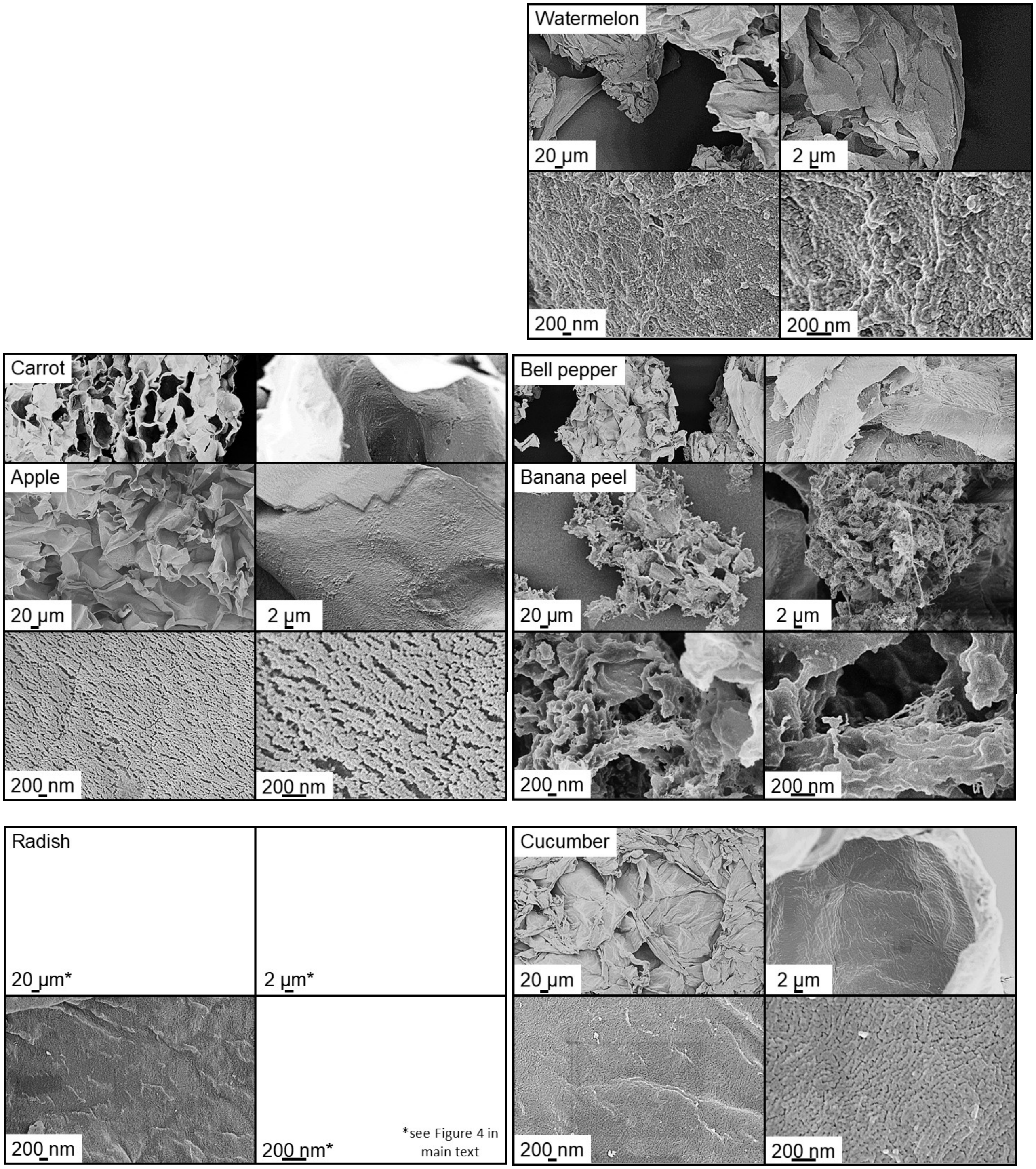

Figure S6: SEM images of all samples, for each individual sample with four different magnifications: 500X, 5000X, 50000X and150000X. Samples are marked with * are shown in the main text.

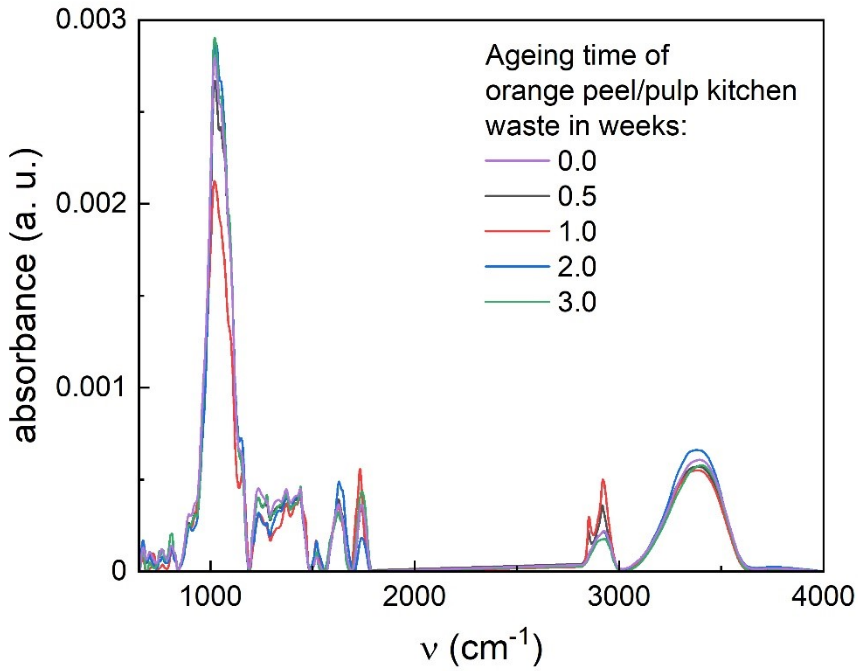

Figure S7: FT-IR spectra of tissue based aerogels which were obtained from kitchen waste after different storage times.

Table S3: List of specific surface areas and densities reported in literature for typical sol-based aerogels produced from cellulose, pectin, proteins via supercritical drying, including sources. References are listed at the end of the SI.

Material (-)	Extracted from (-)	Specific surface area S_m ($m^2 g^{-1}$)	Density ($g\ cm^{-3}$)*	Reference* (-)
Cellulose	n.d.	206, 222, 216, 208, 206, 206, 197, 186, 195, 163, 156, 158, 136, 350, 241, 282, 286, 291, 313, 375, 402, 431, 416, 396, 389, 330, 200, 220, 240, 388, 443, 448	0.08, 0.09, 0.09, 0.10, 0.11, 0.16, 0.17, 0.17, 0.17, 0.20, 0.20, 0.22, 0.22, 0.23, 0.23, 0.24, 0.24, 0.25, 0.25, 0.26, 0.27, 0.27, 0.27, 0.30, 0.01, 0.02, 0.02, 0.03, 0.04, 0.04, 0.05, 0.05, 0.06, 0.08, 0.10, 0.07, 0.13, 0.13, 0.16, 0.17, 0.21, 0.18, 0.10, 0.23,0.03, 0.05, 0.08, 0.10, 0.12, 0.08, 0.10, 0.13; ρ_b	1***
	n.d.	491, 421, 354	0.16, 0.22, 0.28; ρ_e	2
	n.d.		0.06, 0.17, 0.22, 0.24, 0.30, 0.02, 0.04, 0.06, 0.09, 0.10; ρ_e	3
	n.d.	172, 284	0.05, 0.26; ρ_b	4
	n.d.	539	0.05; ρ_b	5
	n.d.	384, 380, 371	0.08, 0.10, 0.11; ρ_e	6
	n.d.	289	0.18; ρ_e	7
	n.d.	360, 336, 422, 381	0.06, 0.08, 0.09, 0.11; ρ_b	8
Natural tissues	no extraction	113	0.032; ρ_b	9
	no extraction	208, 229	0.191, 0.016; ρ_b	10
Pectin	Citrus or apple	230, 270		11
	Citrus		0.05, 0.09, 0.12, 0.17; ρ_b	11
	Apple		0.14, 0.08, 0.11; ρ_b	11
	Citrus	554, 593, 249, 143		12
	Apple	469, 515, 214		12
	n.d.	718, 710, 627	0.04, 0.07, 0.09; ρ_e	2
	Citrus	441	0.08; ρ_b	13

	Citrus	362	0.08; ρ_b	14
	Watermelon	524, 585	0.05, 0.07; ρ_b	15
	Citrus	469, 527, 525, 523, 537, 523,	0.03, 0.03, 0.06, 0.04, 0.04, 0.10; ρ_b	15
	n.d.	461	0.11; ρ_b	16
	n.d.	528, 595, 558		17
	Citrus	397		18
Proteins	Whey	65		19
	Whey		0.02; ρ_b	20
	Egg	375, 358, 234, 231, 27, 16, 176, 160, 211, 187, 242, 209	0.04, 0.04, 0.03, 0.02, 0.02, 0.02, 0.03, 0.03, 0.04, 0.04, 0.05, 0.05; ρ_b	21
	Potatoes	200	0.01; ρ_e	7
	Whey	201	0.01; ρ_e	7
	Whey	412, 422, 384, 390		22
	Egg	378, 220, 291, 359		22
	Potatoes	459, 337, 311, 271, 175		23
	Whey	477, 370, 355	0.14, 0.15, 0.18; ρ_b	24
	Potatoes	479, 347, 403	0.08, 0.11, 0.10; ρ_b	24
	Whey	416, 447, 14, 327, 310, 388	0.38, 0.43, 0.30, 0.39, 0.38, 0.37; ρ_b	25

* Includes bulk (ρ_b) and envelope (ρ_e) densities.

** The specific surface area and densities are only assigned to the source and are not related to each other, although they are listed in the same line.

*** The review was cited instead of the primary sources.

Environmental assessment

Table S4: Mass flow for conventional sol-gel regeneration process. To estimate the consumption of carbon dioxide, the lab-scale process established in out lab has been used: the volume of the autoclave is 250 mL; filling of the autoclave is 0.75; skeletal density of the aerogel 1.50 g/mL; CO_2 flowrate 20.00 g min^{-1}; duration of drying is 180 min.

Component	Mass used [g]	Mass disposed [g]	Comment
NaOH	6.58	6.58	
urea	11.28	11.28	
water, dissolution	76.14	76.14	
cellulose microcrystalline	6.00	0.00	6wt% solution of cellulose
H_2SO_4	5.00	5.00	1:1 w/w ratio between cellulose solution and regeneration bath assumed
water, regeneration	95.00	95.00	
water, washing	3600.00	3600.00	Calculated with a washing factor of 600 (equal to mass of water needed for washing of 1 g of polymer)
ethanol, solv.exch.	564.00	564.00	6 steps SE with (100-mass of cellulose) g pure EtOH
CO_2 drying	76.80	76.80	3 h drying at 20 g/min CO_2 consumption
water TOTAL	3771.14	3771.14	

Table S5: Mass flow for the process reported in this work. Assumptions: the mass of biomass is 500 g; water-insoluble fraction is 0.10 (this fraction is fully converted into aerogel); water-soluble fraction is 0.10 (sugars, organic acids, vitamins, minerals, and soluble fibers); water fraction in the biomass is 0.80.

Component	Mass used [g]	Mass disposed [g]	Comment
NaOH	0.00	0.00	
urea	0.00	0.00	
water, dissolution	500.00	500.00	water for making the biomass loose
water-insoluble fraction	50.00	0.00	water-insoluble fraction (it gets converted into aerogel)
H2SO4	0.00	0.00	
water, regeneration	0.00	0.00	
water, washing	30000.00	30000.00	three times 10 L. This amount of water corresponds to a washing factor of 600
ethanol, solvent exchange	2250.00	2250.00	5 steps SE with pure EtOH (= 5x the mass of water-insoluble fraction)
CO_2 for drying	640.00	640.00	3 h drying at 20 g min^{-1} CO_2 consumption
water TOTAL	30500.00	30900.00	extra water from fruit is added to the mass disposed
Soluble fraction	0.00	50.00	

Table S6: Environmental indices for conventional sol-gel regeneration process.

Component	Environmental index, input, g/g	Environmental index, output, g/g
sodium hydroxide	0.52	0.44
urea	0.42	0.75
water	0.00	0.00
cellulose microcrystalline	0.08	0.00
sulfuric acid	0.54	0.69
ethanol	21.15	28.20
carbon dioxide	0.00	4.16
EI Process	**56.95**	
EI (Process, in & out)	**22.71**	**34.24**
GEI (in & out)	**0.03**	**0.05**

Table S7: Environmental indices for the process reported in this work.

Component	Environmental index, input, g/g	Environmental index, output, g/g
water TOTAL	0.000	0.000
water-insoluble fraction	0.000	0.000
ethanol	10.125	13.500
carbon dioxide	0.000	4.160
soluble fraction	0.000	0.000
EI Process	**27.79**	
EI (Process, in & out)	**10.13**	**17.66**
GEI (in & out)	**0.02**	**0.03**

Table S8: Impact categories for the components used in the conventional sol-gel and novel processes.

Component	Raw Material Availability	Complexity of the Synthesis	Critical Materials Used	Thermal Risk	Acute Toxicity	Chronic Toxicity	Endocrine Disruption	GWP	Ozone Depletion Potential	Acidification Potential	Photochemical Ozone Creation Potential	Odor	Eutrophication Potential	Organic Carbon Pollution Potential
NaOH	B	B	B	B	A	B	C	B	C	B	C	C	C	C
Urea	B	B	B	C	B	B	C	B	C	B	C	B	A	B
Insoluble fraction	C	C	C	C	C	C	C	C	C	C	C	C	C	C
Microcrystalline cellulose	C	B	B	C	C	C	C	C	C	B	C	C	C	C
H2SO4	B	B	B	A	A	A	C	B	C	A	C	B	B	B
Water	C	C	C	C	C	C	C	C	C	C	C	C	C	C
Ethanol for solvent exchange	C	B	C	B	B	B	C	C	C	C	B	B	C	B
CO_2 for drying	C	C	C	C	C	C	C	A	C	B	C	C	B	B
Soluble fraction	C	C	C	C	C	C	C	C	C	C	C	C	C	C

The classification of chemicals into categories A (most harmful or significant effect), B (moderate effect), and C (no harm or no effect) was based on a comprehensive evaluation of their environmental, health, and safety impacts:

- **Raw material availability** was assessed based on natural abundance and renewability, with biogenic substances such as cellulose receiving a C rating, whereas chemicals derived from non-renewable sources or requiring complex synthesis were rated B or A.
- **Complexity of synthesis** considered the number of processing steps, energy demand, and reliance on hazardous reagents, leading to higher ratings for chemicals involving extensive purification or transformation.
- **Critical materials used** focused on substances requiring rare, toxic, or environmentally sensitive precursors.
- **Thermal risk** accounted for stability under standard conditions, with volatile or exothermically decomposing substances assigned a higher risk rating.
- **Acute and chronic toxicity** classifications were based on known toxicological profiles, occupational exposure limits, and regulatory assessments, with highly toxic substances categorized as A.
- **Endocrine disruption** was considered based on known or suspected interference with hormonal systems.
- **Global warming potential (GWP), ozone depletion, acidification, and photochemical ozone creation** were evaluated using established environmental impact metrics, where substances contributing significantly to greenhouse gas emissions or atmospheric reactions were rated A.
- **Odor, eutrophication potential, and organic carbon pollution potential** were assessed based on sensory perception, nutrient pollution risks, and persistence in the environment, respectively. This structured classification enables a systematic comparison of chemicals, facilitating informed decision-making in process development and environmental impact mitigation.

Figure S8: Images of different tissue based aerogel particles mixed with increasing amounts of sunflower oil. The ratios given in the insets corresponds to the weight ratio of aerogel : oil. Red highlighted insets mark the minimum oil content oil_{gel} at which the transition from a granular solid to a continuous self-standing oleogel occurs.

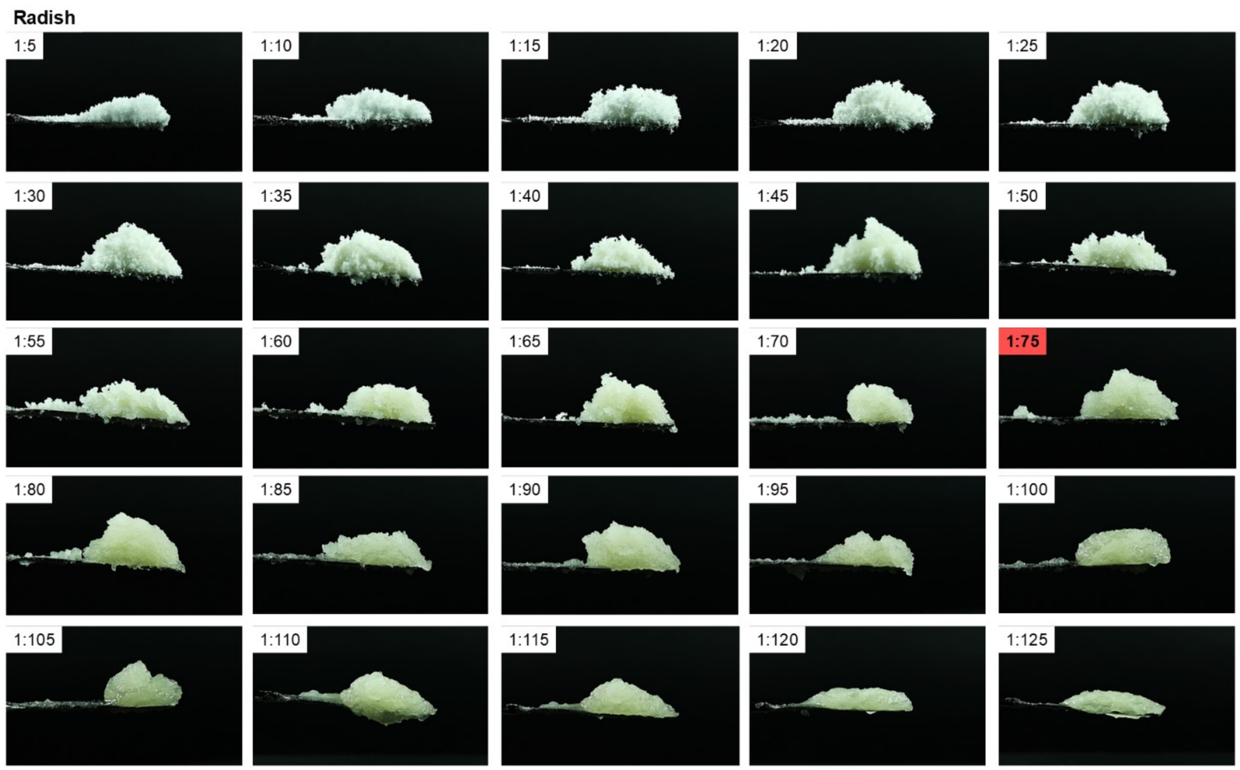

Figure S9: Images of radish based aerogel particles mixed with increasing amounts of sunflower oil. The ratios given in the insets corresponds to the weight ratio of aerogel : oil. Red highlighted insets mark the minimum oil content oil_{gel} at which the transition from a granular solid to a continuous self-standing oleogel occurs.

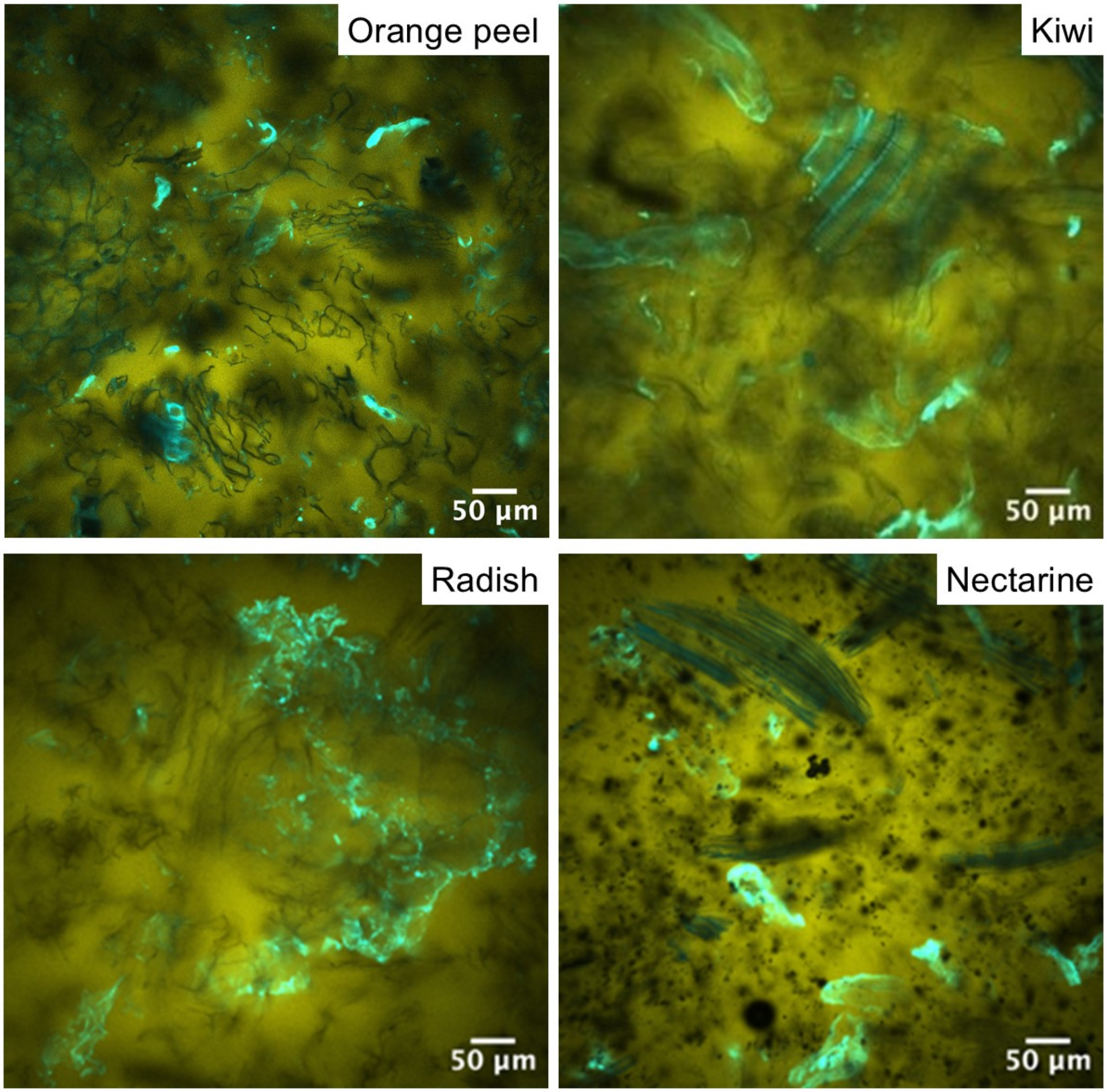

Figure S10: Additional confocal micrographs of oleogels based on different tissue-based aerogels.

Reference list for **Table S3**.

1 T. Budtova, *Cellulose*, 2019, **26(1)**, 81–121.
2 A. Rege, I. Preibisch, M. Schestakow, K. Ganesan, P. Gurikov, B. Milow, I. Smirnova, and M. Itskov, *Materials*, 2018, **11(9)**, 1670.
3 A. Rege, M. Schestakow, I. Karadagli, L. Ratke, and M. Itskov, *Soft Matter*, 2016, **12(34)**, 7079–7088.
4 F. Liebner, A. Potthast, T. Rosenau, E. Haimer, and M. Wendland, *Holzforschung*, 2008, **62(2)**, 129–135.
5 Aaltonen and O. Jauhiainen, *Carbohydr. Polym.*, 2009, **75(1)**, 125–129.

6 F. Ciuffarin, M. Négrier, S. Plazzotta, M. Libralato, S. Calligaris, T. Budtova, and L. Manzocco, *Food Hydrocoll.*, 2023, **140**, 108631.
7 B. Schroeter, I. Jung, K. Bauer, P. Gurikov, and I. Smirnova, *Polymers*, 2021, **13(17)**, 3000.
8 B. Schroeter, V. P. Yonkova, N. A. M. Niemeyer, I. Jung, I. Preibisch, P. Gurikov, and I. Smirnova, *Cellulose*, 2021, **28(1)**, 223–239.
9 S. Plazzotta, S. Calligaris, and L. Manzocco, *Innov. Food Sci. Emerg. Technol.*, 2018, **47**, 485–492.
10 G. Gaggero, R. P. Subrahmanyam, B. Schroeter, P. Gurikov, and M. Delucchi, *Gels*, 2022, **8(11)**, 691.
11 C. Rudaz, R. Courson, L. Bonnet, S. Calas-Etienne, H. Sallée, and T. Budtova, *Biomacromolecules*, 2014, **15(6)**, 2188–2195.
12 A. Veronovski, G. Tkalec, Ž. Knez, and Z. Novak, *Carbohydr. Polym.*, 2014, **113**, 272–278.
13 M. Pantić, G. Horvat, Ž. Knez, and Z. Novak, *Molecules*, 2020, **25(5)**, 1187.
14 S. Groult, S. Buwalda, and T. Budtova, *Eur. Polym. J.*, 2021, **149**, 110386.
15 D. A. Méndez, B. Schroeter, A. Martínez-Abad, M. J. Fabra, P. Gurikov, and A. P. López-Rubio, *Carbohydr. Polym.*, 2023, **306**, 120604.
16 A. Nešić, M. Gordić, S. Davidović, Ž. Radovanović, J. Nedeljković, I. Smirnova, and P. Gurikov, *Carbohydr. Polym.*, 2018, **195**, 128–135.
17 I. Preibisch, P. Niemeyer, Y. Yusufoglu, P. Gurikov, B. Milow, and I. Smirnova, *Materials*, 2018, **11(8)**, 1287.
18 C. A. García-González, M. Jin, J. Gerth, C. Alvarez-Lorenzo, and I. Smirnova, *Carbohydr. Polym.*, 2015, **117**, 797–806.
19 S. Plazzotta, I. Jung, B. Schroeter, R. P. Subrahmanyam, I. Smirnova, S. Calligaris, P. Gurikov, and L. Manzocco, *Polymers*, 2021, **13(23)**, 4063.
20 S. Plazzotta, S. Calligaris, and L. Manzocco, Structural Characterization of Oleogels from Whey Protein Aerogel Particles, *Food Res. Int.*, 2020, **132**, 109099.
21 I. Selmer, C. Kleemann, U. Kulozik, S. Heinrich, and I. Smirnova, *J. Supercrit. Fluids*, 2015, **106**, 42–49.
22 C. Kleemann, R. Schuster, E. Rosenecker, I. Selmer, I. Smirnova, and U. Kulozik, *Food Hydrocoll.*, 2020, **101**, 105534.
23 D. J. Andlinger, A. C. Bornkeßel, I. Jung, B. Schroeter, I. Smirnova, and U. Kulozik, *Food Hydrocoll.*, 2021, **112**, 106305.
24 I. Jung, B. Schroeter, S. Plazzotta, L. De Berardinis, I. Smirnova, P. Gurikov, and L. Manzocco, *Food Hydrocoll.*, 2023, **142**, 108758.
25 M. Betz, C. A. García-González, R. P. Subrahmanyam, I. Smirnova, and U. Kulozik, *J. Supercrit. Fluids*, 2012, **72**, 111–119.